Anal. Chem. 1995, 67, 777–783

Raman Spectroscopy of Normal and Diseased Human Breast Tissues

Christopher J. Frank† and Richard L. McCreery*

Department of Chemistry, The Ohio State University, 120 West 18th Avenue, Columbus, Ohio 43210

Douglas C. B. Redd

Department of Radiology, Section of Interventional Radiology, University of Pennsylvania School of Medicine, 3400 Spruce Street, 1 Silverstein, Philadelphia, Pennsylvania 19104

Raman spectra of histologically normal human breast biopsy samples were compared to those exhibiting infiltrating ductal carcinoma (IDC) or fibrocystic change. Experiments at 784 nm with CCD detectors reduced fluorescence interference and produced high SNR spectra with relatively low (10–200 mW) laser power. Sample to sample and patient to patient variation for normal specimens were less than 5% for the ratios of major Raman bands. The Raman spectra changed dramatically in diseased specimens, with much weaker lipid bands being evident. The spectrum of infiltrating ductal carcinoma samples is similar to that of human collagen. Differences between benign (fibrocystic) and malignant (IDC) lesions were smaller than those between normal and IDC specimens, but were still reproducible. Fiber-optic sampling through a hypodermic needle and with a remote probe were demonstrated. The possibility of rapid diagnosis with Raman spectroscopy is considered.

Breast cancer represents the most commonly diagnosed cancer in women in the United States and other industrialized nations and accounted for 18% of female cancer deaths in the United States in 1994.[1] While screening mammography has been shown to reduce the mortality from breast cancer by 20%–39% among women aged 50 years and older,[2] the age-adjusted mortality rate for breast cancer has remained stable over the past 40 years, remaining at ~26 per 100 000.[3] Improvements in film-screen mammography now permit reliable detection of very small invasive cancers with prognosis of long-term survival (13 years) greater than 90%.[4] Breast cancers smaller than 1 cm in size have a very low rate of axillary nodal metastasis, which serves as the single most important prognostic indicator of disease-free survival.[5] In order to further characterize an abnormality detected mammographically, tissue sampling procedures like fine-needle aspiration, core biopsy, and excisional biopsy are performed in order to obtain tissue for cytological or histopathological analysis. An estimated 500 000 breast biopsy procedures will be performed in the United States in 1995, with 60%–90% of biopsies performed on the basis of abnormal mammograms revealing benign disease.[6] Thus, there has been criticism of public health policy which utilizes mammography in mass screening programs, due to the high cost per malignancy detected and the accompanying physical and psychological trauma.

Medical diagnostic techniques useful for breast cancer screening include clinical breast examination, breast self-examinations, and screening mammography. While routine film-screen mam-

† Present address: Procter and Gamble Pharmaceuticals, P.O. Box 191, Norwich, New York 13815.

(1) Boring, C. C.; Squires, T. S.; Tony, T.; Montgomery, S. Cancer Statistics 1994. *Ca-A J. Clin.* **1994**, *44*, 7–26.

(2) O'Malley, M. S.; Fletcher, S. W.; Morrison, B. *Does screening for breast cancer save lives? Effectiveness of treatment after breast cancer detection following screening by clinical breast examination, mammography and breast self-examination*; Springer-Verlag: New York, 1990.

(3) National Cancer Institute. *Annual cancer statistics review including cancer trends: 1950–1985.*; U.S. Department of Health and Human Services, PHS, NIH, NCI, 1990.

(4) Tabar, L.; Fagerber, G.; Duffy, S. W.; Day, N. E.; Gad, A.; Grontoft, O. *Radiol. Clin. North Am.* **1992**, *30*, 187–210.

(5) Shek, L. L. M.; Godolphin, W. *Cancer Res.* **1988**, *48*, 5565–5569.

(6) Hall, F. M.; Storella, J. M.; Silverstone, D. Z.; Wysshak, G. *Radiology* **1988**, *167*, 353–358.

0003-2700/95/0367-0777$9.00/0

mography is recognized as highly sensitive for detecting cancer, its findings are frequently nonspecific, thus the high incidence of benign disease upon breast biopsy. Additionally, this modality is of limited value in the case of dense breast tissue, which is encountered in 30%–60% of women[7] or within the posttherapeutically altered breast. Future advances in magnetic resonance imaging (MRI) including the use of contrast-enhanced examinations with specialty breast surface coils offer future promise in breast cancer diagnosis. In addition to information relating to spatial extent of disease with high resolution, application of magnetic resonance spectroscopic techniques may yield information related to biochemical composition.[8-10]

Thus, tissue sampling techniques (e.g., fine needle aspiration, core biopsy, and surgical excisional biopsy) must be relied upon to provide sufficient tissue for histopathological and immunohistochemical analysis. These standard methods provide valuable clinical information but require time-consuming tissue processing and, with the exception of frozen section analysis, are not routinely available during surgery, nor are they amenable to in vivo use.

Vibrational spectroscopy offers attractive features (e.g., Raman and IR absorption contain detailed information relating to molecular structure and composition) but are not yet used to a significant extent in a clinical setting. Recent technical developments now permit compact, portable spectrometers which can provide spectra in a few seconds. While not as specific as antibody-based immunohistochemical methods, vibrational spectroscopic techniques do offer complementary information, not available from X-ray or MRI techniques, which may be of clinical value in diagnosis.

Several reports have appeared on the Raman spectroscopy of normal and diseased tissue, with the long-range objective of medical diagnosis. Our laboratory examined normal human breast biopsy samples with Raman spectroscopy[11] and demonstrated that high signal to noise ratio (SNR) spectra could be obtained at low laser power (~40 mW) and with the flexibility of fiber-optic sampling. The effort reported here was directed toward characterizing lesions in breast tissue by Raman spectroscopy. The principal issue was whether the molecular information available from Raman spectroscopy could provide a diagnostically useful signature associated with abnormality. If so, Raman spectroscopy might provide a rapid and minimally invasive method of medical diagnosis of breast disease and potentially other disorders.

EXPERIMENTAL SECTION

The Raman spectrometer was the same as that described previously.[11] A 640 mm single spectrograph and 1152 × 296 pixel CCD detector were preceded by a holographic band reject filter and 180° backscattered collection geometry. A Ti:sapphire laser operating at 784 nm was filtered by a holographic band pass filter and delivered 20–100 mW at the sample. The Raman shift axis was calibrated with a second-order fit to known frequencies (naphthalene and toluene/acetonitrile), and is accurate to ±2 cm^{-1}. The intensity scale was corrected for instrument response function with a white light source as described elsewhere.[12] The Photometrics software (CCD 9000) permitted summing of successive integrations, and spectra were often obtained by adding several 2 min integrations (as noted).

A fiber-optic needle probe was constructed according to a previous design,[13] with one laser fiber surrounded by six collection fibers. One meter lengths of 200 μm fiber (Ensign-Bickford) were stripped of their jackets (with the cladding remaining intact) over the final 40 mm. The 6 × 1 array was embedded in a 1 mm i.d. core biopsy needle with Torr-seal (Varian) and polished after curing. The six collection fibers were positioned at the slit image of the spectrograph, such that the collected light passed through the holographic filter before entering the spectrograph. The 6 × 1 probe was tested with a liquid sample and exhibited performance qualitatively similar to that reported for a 18 × 1 array[13] and a commercial Raman system.[14] The 6 × 1 probe sampled ~0.5–5 mm into a clear liquid sample.

An integrated fiber-optic probe from Detection Limit Technologies (DLT, Laramie, WY) was interfaced to a Chromex Raman One system (Albuquerque, NM) with a 512 × 512 back-thinned CCD. The probe contained band pass and band reject filters (782 nm) which permitted long fiber lengths (50 ft) to be used. The probe also used 180° backscattered geometry, with the focus ~40 mm from the 2 in. × 2 in. probe body. Except for those obtained with the DLT probe and Chromex spectrograph, all spectra were obtained with the ISA/EEV system described previously.[11] Internal probe luminescence was corrected by subtracting a spectrum of air from tissue spectra obtained with the DLT probe.

Normal breast tissue specimens were obtained following surgical excision in patients undergoing reduction mammoplasty, excisional biopsy, or modified radical mastectomy. In the latter two groups, tissue provided for spectroscopy was selected from areas near the surgical margins and several centimeters from the tumor prompting the surgical procedures and was documented as normal by a staff pathologist. All tissue samples were obtained from patients who preoperatively signed an informed consent permitting the investigational use of tissues under guidelines approved by the university Institutional Review Board. To minimize any possible changes in the tissue with time, data presented here were acquired within a 72 h period. All samples were stored in a solution of 10% formalin with 50 mM phosphate buffer (pH 6–7) and run at an ambient temperature of 22 ± 1 °C.

RESULTS

A critical issue for useful diagnosis is the requirement that variations in spectra from normal biopsy specimens be smaller than those occurring between normal and abnormal tissue. The standard deviation for run to run, sample to sample, and patient to patient variations must be small compared to a change caused by an abnormality. Accordingly, a broad range of normal samples was examined to assess this variation. In this context, "normal" is defined as tissue that shows no signs of abnormality as judged by a pathologist. While the sample may have come from a patient with a disorder (as indicated), the tissue was from a location that was deemed histopathologically normal. A Raman spectrum of normal human breast tissue is shown in Figure 1A, and a more

(7) Sabol, J. M.; Soutar I.; Plewes, D. B. *Med. Phys* **1993**, *20*, 1505–15.
(8) Victor, T. A.; Bergman, A.; Knop R. H. *Br. J. Cancer* **1993**, *68*, 336–41.
(9) Kalra, R.; et al. *Br. J. Cancer* **1993**, *67*, 1145–53.
(10) Bradamante, S.; Barchiesi, E.; Pilotti, S.; Borasi, G. *Magn. Reson. Med.* **1988**, *8*, 440–9.
(11) Frank, C. J.; Redd, D. C. B.; Gansler, T. S.; McCreery, R. L. *Anal. Chem.* **1994**, *66*, 319–26.
(12) Fryling, M. A.; Frank, C. J.; McCreery, R. L. *Appl. Spectrosc.* **1993**, *47*, 1965.
(13) Schwab, S. B.; McCreery, R. L. *Anal. Chem.* **1984**, *56*, 2199–204.
(14) Newman, C. D.; Bret. G. C.; McCreery, R. L. *Appl. Spectrosc.* **1992**, *46*, 262–5.

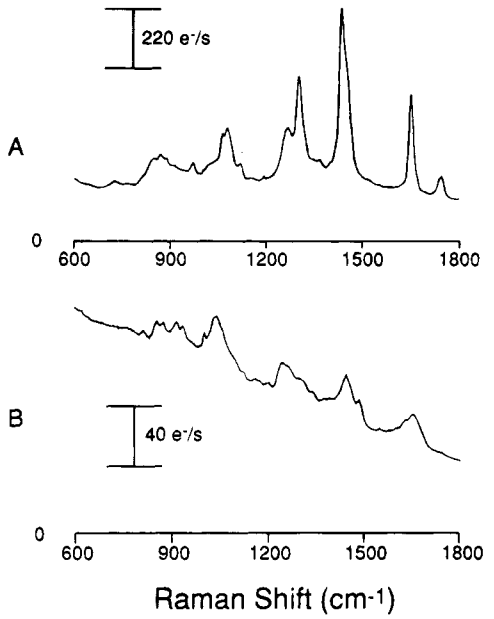

Figure 1. Raman spectra of breast biopsy tissue obtained with 180° backscattered geometry, 784 nm laser wavelength: (A) normal tissue, 3.4 cm^{-1} band pass, 100 mW, and 300 s integration; (B) infiltrating ductal carcinoma, 200 mW, 1.7 cm^{-1} band pass, and 600 s. *X*-axis represents zero scattered intensity in both spectra.

Table 1. Peak Frequencies (cm^{-1}) for Raman features

normal tissue[a]	oleic acid methyl ester	infiltrating ductal carcinoma	type 1 collagen (human placenta)	collagen assignments[18]
		817	814	C–C stretch
727	728	856	855	C–C stretch, proline
870	868	876	874	C–C stretch, hypro[b]
		920	920	C–C, proline ring
972	973	937	934	C–C, backbone
		1004	1002	phenylalanine
1066	1067	1043	1032	proline
1079	1082	1125	1127	
1119	1118	1167	1166	
		1206	1206	hypro, tyrosine
		1247	1247	amide III
1265	1268	1267	1269	amide III
1303	1304	1303	1319	CH_3, CH_2, twist
		1343	1343	CH_3, CH_2, wag
1439	1442	1450	1451	CH_3, CH_2 deform
		1554	1554	
1654	1655	1657	1665	amide I
1743	1743			

[a] All spectra listed were obtained with a 784 nm laser wavelength. [b] Hydroxyproline.

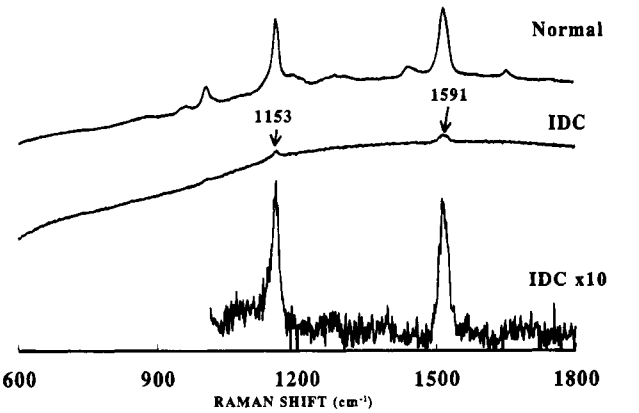

Figure 2. Raman spectra of normal and IDC specimens obtained with 50 mW of 514.5 nm laser light, 2 s integration time, and 2.0 cm^{-1} band pass. Lower spectrum is magnified and baseline subtracted.

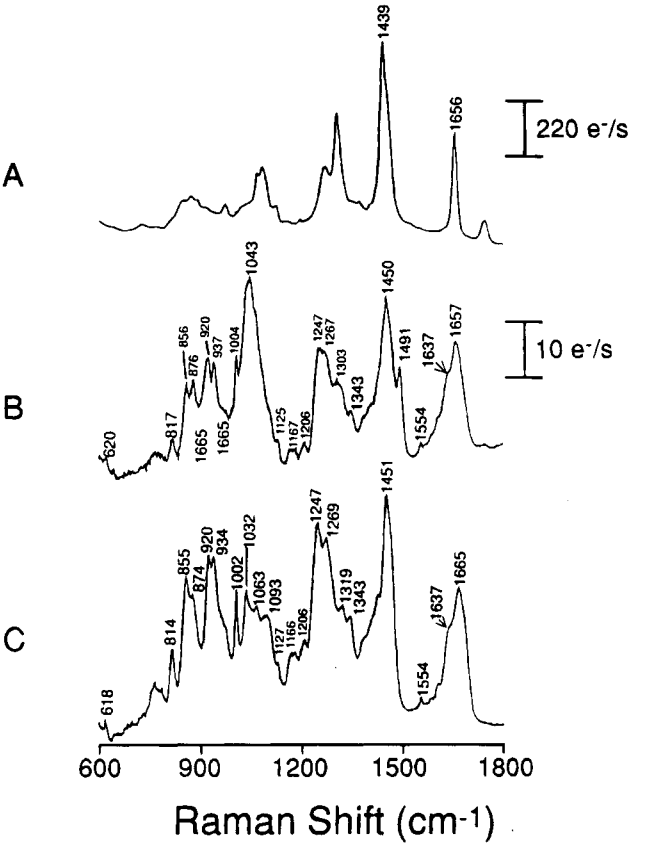

Figure 3. Raman spectra (784 nm) 100 mW at sample, 300 s integration time: (A) normal tissue; (B) IDC; (C) type I collagen from human placenta, average of 36 2 min integrations. Sloping background was subtracted from spectra B and C.

detailed spectrum is in ref 11, Figure 4. The 784 nm laser wavelength yields low fluorescence background, and the spectral features are attributable to lipids, mainly an oleic acid derivative. Table 1 lists the observed bands, and assignments are summarized in ref 11. The carotenoid bands are notably absent with the 784 nm laser due to lack of resonance enhancement.[15]

The area ratio of the 1654–1439 cm^{-1} band was chosen for quantitative comparison because both bands are sensitive to histopathological abnormality, as shown below. The 1654 nm band (C=C stretch) intensity varies with the degree of fatty acid unsaturation, and the 1439 cm^{-1} band (CH_2 scissoring) depends on the lipid to protein ratio. To evaluate variation of the 1654/1439 cm^{-1} band area ratio, spectra were obtained from three different locations on each of three specimens from the same patient. In addition, biopsies from 12 patients were compared, and for three patients, the left breast biopsy was compared to the right. In addition to the 1654/1439 band area ratio, the Raman/fluorescence (R/F) ratio was compared, defined as the peak height of the 1439 cm^{-1} band divided by the baseline fluorescence intensity at 1200 cm^{-1}. The results are shown in Tables 2 and 3 for a total of 123 spectra from 41 specimens from 12 patients. Since repeated spectra of the same spot showed a standard deviation

(15) Redd, D. C. B.; Feng, Z. C.; Yue, K. T.; Gansler, T. S. *Appl. Spectrosc.* **1993**, *47*, 787–91.

Table 2. Summary of 1654/1439 cm^{-1} Band Area and 1439 cm^{-1} R/F Ratios for 784 nm Raman Spectra of Normal Breast Tissue from Patients with Varying Ailments[a]

patient	diagnosis[b]	age	no. of specimens[c]	no. of spectra[d]	1654/1439 cm^{-1}[e]	R/F[f]
1-R[g]	reduction	47	3	9	0.32 ± 0.01 (3.4)	2.6 ± 0.5 (19)
1-L	reduction	47	3	9	0.31 ± 0.01 (3.6)	2.0 ± 0.3 (16)
2-R	reduction	17	3	9	0.28 ± 0.02 (7.1)	2.0 ± 1.2 (63)
2-L	reduction	17	3	9	0.27 ± 0.01 (4.5)	2.6 ± 1.1 (41)
3-R	reduction	19	2	6	0.25 ± 0.01 (5.1)	3.1 ± 0.3 (11)
3-L	reduction	19	3	9	0.25 ± 0.01 (3.2)	1.9 ± 0.8 (41)
4	CA	63	3	9	0.30 ± 0.01 (3.2)	2.2 ± 0.3 (15)
5	CA	50	3	9	0.34 ± 0.02 (4.7)	1.4 ± 0.6 (41)
6	IDC	45	3	9	0.26 ± 0.01 (4.9)	2.0 ± 0.7 (35)
7	IDC	67	3	9	0.27 ± 0.04 (14)	2.3 ± 0.8 (37)
8	IDC	55	3	9	0.26 ± 0.01 (3.2)	1.7 ± 0.7 (39)
9	CA	61	3	9	0.32 ± 0.01 (3.8)	2.3 ± 0.3 (11)
10	CA	53	2	6	0.30 ± 0.01 (4.1)	1.6 ± 0.5 (30)
11	CA	40	3	9	0.27 ± 0.01 (3.4)	1.9 ± 0.4 (24)
12	CA	47	1	3	0.26 ± 0.02 (6.8)	1.8 ± 0.7 (38)

[a] See ref 25, Appendix 1 for more detailed listing. [b] Reason for surgical procedure that produced these specimens: reduction, breast reduction; IDC, infiltrating ductal carcinoma; CA, breast cancer. [c] Number of specimens; three Raman spectra were obtained from different locations on each specimen. [d] Number of spectra. [e] Band area ratio. Numbers in parentheses are RSD(%). [f] Ratio of intensity of 1439 cm^{-1} band to fluorescence intensity at 1200 cm^{-1}. Numbers in parentheses are RSD(%). [g] *R*, right breast; L, left breast.

Table 3. Statistics for 1654/1439 cm^{-1} Band Area Ratio for 784 nm Raman Spectra of Normal Breast Tissue

	RSD,[a] %	*N*
same spot	1.5	12
different spots (same specimen)	3	9
different specimens (same patient)	4	9 spectra, 3 specimens
different breast cases		
reduction	4.5	6 breast cases, 3 patients, 51 spectra
breast cancer	5.3	9 breast cases, 9 patients, 72 spectra
both	5	15 breast cases, 12 patients, 123 spectra

[a] Relative standard deviation.

of 1.5%, most of the variation observed is biochemical rather than instrumental. It should be emphasized that the discussion thus far is for histologically normal tissue from breast reduction and cancer cases and does not include any tissue known to be abnormal.

Figure 1 compares a normal spectrum to one obtained from a lesion identified as infiltrating ductal carcinoma (IDC). Taking the differences in scale into account, the IDC spectrum is much weaker than that from a normal sample (with principal Raman features ~5% as intense as the "normal" 1439 cm^{-1} band) and obvious qualitative changes are apparent. Raman spectra of normal and IDC tissue obtained with a 515 nm laser are shown in Figure 2 and show mainly carotenoid features. Both the lipid and carotenoid bands are superimposed on relatively intense fluorescence, and the changes in the IDC spectrum are less obvious. The lower background and higher SNR obtained with the 784 nm laser is a clear advantage of the near-IR Raman technique. Higher SNR spectra obtained with more near-IR laser power and longer integration time are shown in Figure 3, and the observed peak positions are listed in Table 1. The Raman spectrum of type I collagen from human placenta is included in Figure 3 for comparison.

The shift of the prominent 1439 cm^{-1} feature in normal tissue to 1450 cm^{-1} in IDC is reproducible and significant and is attributable to the different CH_2 deformation frequencies in fatty acids and proteins. Collagen is a structural protein, which occurs in several forms.[16,17] The band assignments of Frashour and Koenig[18] are included in Table 1. Raman spectra of four types of collagen from human placenta are shown in Figure 4.

Increased collagen formation may also be present in benign conditions of the breast, e.g., fibrocystic change, a condition commonly encountered in older women. A comparison of spectra from two IDC specimens from the same patient and a specimen with fibrocystic change is shown in Figure 5. While the IDC and FC spectra are similar, there are some reproducible differences. The FC spectrum has smaller amide I (1656 cm^{-1}) and amide III (1259 cm^{-1}) intensities relative to the 1449 cm^{-1} CH_2 deformation band, and the CH_2 deformation is at lower frequency (1446 vs 1449 cm^{-1}). In addition, the structure in the 850–950 cm^{-1} region differs, with only two peaks resolved in the FC case and four in IDC. Although these differences may be diagnostically useful, too few samples have been evaluated to determine their statistical significance.

All data discussed thus far was obtained with the 180° "epi" geometry described previously.[11] While this sampling mode is fast and convenient for biopsy samples, it is not amenable to remote sampling. For example, a surgeon or pathologist may wish to examine a specimen immediately in the operating room, perhaps in vivo. We reported earlier on an "18 × 1 parallel" fiber-optic probe that obtained spectra 0.5 m away from a compact

(16) al-Adnani M. S.; Taylor, S.; al-Bader, A. A.; al-Zuhair, A. G.; McGee, J. O. *Histol. Histopathol.* **1987**, *2*, 227–38.
(17) Verhoeven, D.; Van Marck, E. *Pathol. Res. Pract.* **1993**, *189*, 851–61.
(18) Frushour, B. G.; Koenig, J. L *Biopolymers* **1975**, *14*, 379–91.

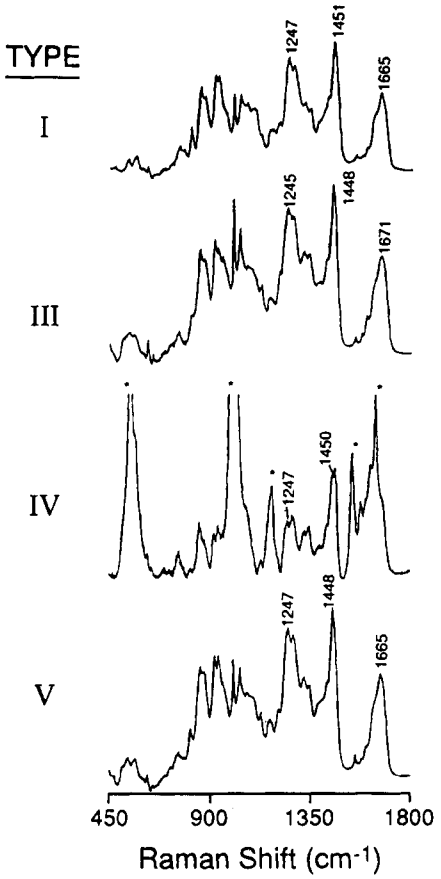

Figure 4. Raman spectra (784 nm, 200 mW) of four types of collagen from human placenta. Sloping baseline was subtracted in all cases. Asterisks in type IV spectrum are due to solubilizing agent. Twenty-five 2 min spectra were averaged.

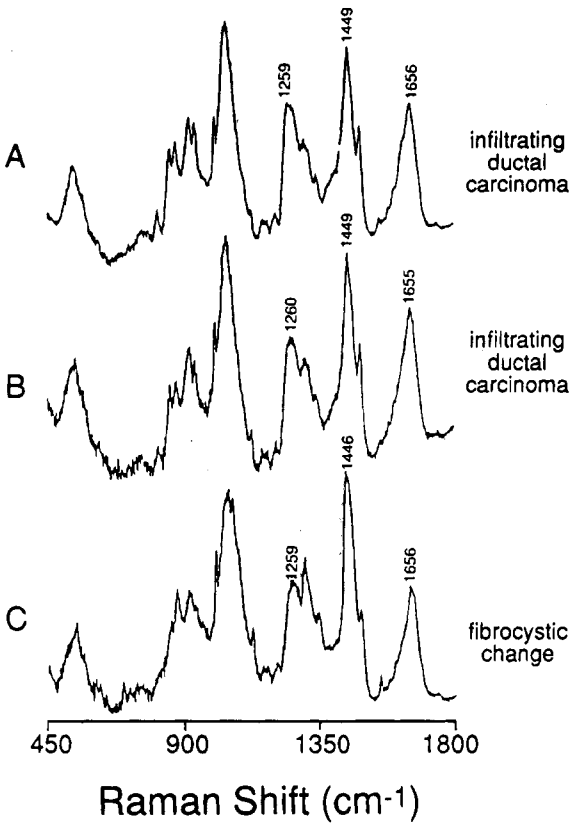

Figure 5. Raman spectra (784 nm, 200 mW) of infiltrating ductal carcinoma (A, B) and fibrocystic change (C) after sloping baseline was subtracted. Spectra A and B were from different specimens from the same patient.

spectrometer.[14] A modification of this approach is a 6 × 1 fiber bundle (one for the laser, six for collection) inserted in a 1 mm diameter needle. Figure 6 shows spectra of normal and IDC biopsy specimens obtained with the needle probe positioned above a biopsy sample compared to those obtained with the epi geometry. Other than a silica Raman feature in the IDC spectrum, the spectra are comparable. The needle probe was evaluated on a breast carcinoma model sample consisting of an 11 mm thickness of formalin-fixed normal tissue placed on top of an 8 mm thick tumor specimen. The fiber-optic needle was then inserted into the tissue sample, and the spectra of Figure 7 were recorded. When the needle tip was above and 3 mm into the normal tissue, the expected "normal" lipid spectrum was obtained. When the needle was inserted 1 mm or more into the tumor, the weaker protein spectrum was observed, with the expected shift from 1439 to 1448 cm^{-1} for the CH_2 deformation.

Figure 8 shows spectra obtained with the DLT remote probe, with 50 ft of laser and collection fiber between the probe and the spectrometer. The probe background was subtracted from the tissue spectra after recording a background spectrum with no sample present. Integration time were quite long due to optical losses in the probe and long fibers. Except for reduced SNR, the remote spectra were similar to those obtained with the 180° epi geometry for both normal and IDC tissue.

DISCUSSION

The obvious changes in spectral features and intensities evident in Figures 1, 3, and 5 demonstrate the sensitivity of Raman spectroscopy for characterizing breast tissue, including IDC, breast cancer, and fibrocystic change. The significantly lower background for 784 nm excitation compared to 515 nm improves the SNR and enhances spectral information by minimizing sample fluorescence. The lack of lipid features in the IDC spectrum implies a relative increase in protein content, possibly accompanied by a decrease in sampling depth due to greater scattering by the protein. These spectral changes in IDC and FC mirror changes seen on histopathology where both of these breast lesions are firm and rubbery on gross examination with marked increase in interstitial tissues seen microscopically.

Quantitatively, the spectral changes accompanying IDC are much larger than the variation in normal specimens. The relative standard deviation for 123 "normal" spectra from 12 patients was 5%, while the change in 1654/1439 cm^{-1} ratio was at least 100% in the IDC specimens. Furthermore, all of the normal spectra were quantitatively very similar. Even if the qualitative changes with IDC were ignored, the increase in 1654/1439 cm^{-1} band area ratio with from ~0.3 to ~1.0 would be an obvious warning of abnormality. Based on the rather limited data base of 12 patients, the spectral changes accompanying IDC, breast cancer, or fibrocystic change are reproducible and not subtle.

High SNR spectra were not obtainable with a 515 nm laser (Figure 2) due to high fluorescence background. At 784 nm, however, long integration times and low background permitted observation of numerous bands attributable to collagen. Except for the large feature at 1043 cm^{-1} in the IDC specimens, there is excellent correspondence with type I collagen, and types III and IV differ in the 850–950 cm^{-1} region and the phenylalanine band

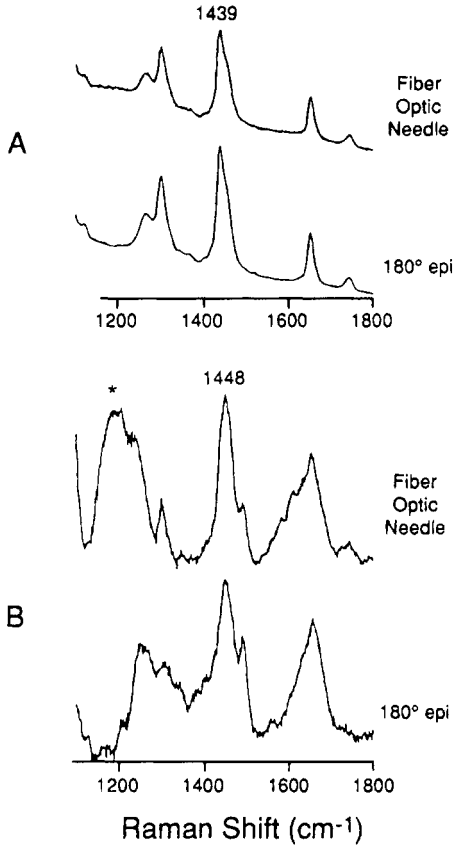

Figure 6. Comparison of Raman spectra from 180° backscattered and 6 × 1 fiber-optic "needle" probe positioned 1 mm above the tissue sample: (A) normal tissue, 60 s, and 75 mW; (B) diseased tissue, average of 50 2 min spectra. Asterisk indicates silica Raman band.

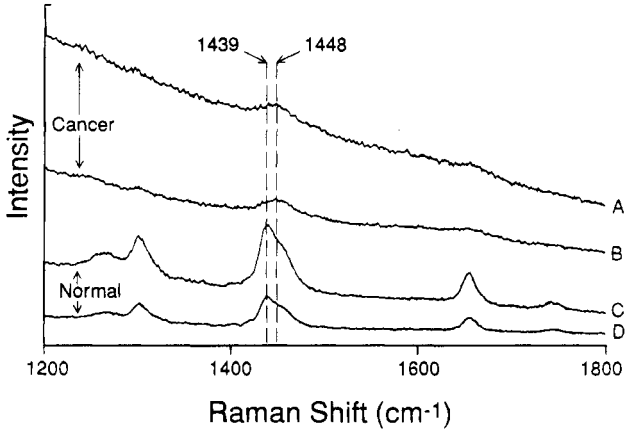

Figure 7. Spectra obtained with 6 × 1 needle probe from a tumor model consisting of 8 mm of normal tissue placed on the surface of an 11 mm deep tumor (100 mW, 60 s). Needle end was (D) 3 mm above the normal tissue, (C) 3 mm into normal tissue, (B) 1 mm into tumor, and (A) >1 mm into the tumor. Spectra were not offset, and intensities reflect absolute values.

intensity at 1004 cm^{-1}. While the similarity of spectra does not prove that type I collagen is present in IDC specimens, the results are consistent with that possibility.

The spectral differences between malignant (IDC) and benign (fibrocystic change) specimens shown in Figure 5 are less obvious, and due to limited tissues for sampling, statistical evaluation could not be performed. However, if the differences in the 850–950 and 1200–1400 cm^{-1} range are larger than patient to patient variations, they might form the basis of a clinical diagnosis. A

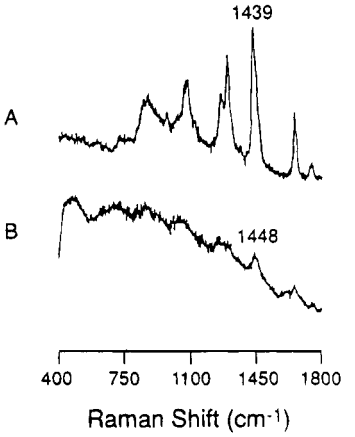

Figure 8. Spectra of normal and diseased tissue obtained with DLT remote probe, with 50 ft of 200 μm fiber-optic probe between probe and spectrograph/laser. Probe background was subtracted after acquiring the spectrum of air: (A) normal tissue, 300 s integration, and 50 mW at sample; (B) IDC, average of 25 3 min integrations.

high-resolution spectrum of the 850–950 cm^{-1} region may reveal consistent differences between malignant and benign tissue that warrant further investigation with large numbers of patients.

Several pathology studies have examined lipid composition of normal and cancerous breast tissue via bulk analysis of excised tissue. Sakai et al. observed a 65% decrease in triglyceride content in cancerous breast tissue compared to normal tissue from the same patient but a 4-fold increase in phospholipids.[19] The relative amounts of unsaturated fatty acids were increased in breast cancer tissues in all the phospholipid subclasses analyzed, particularly for phosphatidylethanolamines.[20] Since triglycerides are much more concentrated than phospholipids in normal tissue, total lipid content decreased significantly in cancerous tissue. The major fatty acid components identified in both healthy and diseased tissue were palmitate, oleate, and linoleate, with the relative proportions in healthy tissue being 1.5:2.7:1.0, respectively.

London et al. confirmed that these fatty acids dominate the fatty acid composition in healthy adipose tissue, with relative proportions of 1.1:2.5:1.0 for palmitic/oleic/linoleic, respectively.[21] Compared with iliac fat, mammary fat is higher in saturated (33.2% vs 24.4%), lower in monounsaturated (48% vs 54.8%), and lower in polyunsaturated fatty acids (16.6% vs 18.0%); thus, breast and iliac fat differ with regard to fatty acid composition.[22] Heitanan et al. also observed a 3.6-fold increase in phospholipid content in cancerous tissue, plus an increase in unsaturated fatty acids.[23] When phospholipid metabolism is observed using ^{31}P magnetic resonance spectroscopy, the in vivo contributions in human breast cancers are predominantly due to phosphatidylethanolamine.[9] Low levels of polyunsaturated fatty acids in breast tumor phosphatidylethanolamine is predictive of early visceral metastasis, and low stearic acid level in breast tumor phosphatidylcholine is predictive of subsequent metastasis.[24] Thus, the involvement of lipid

(19) Sakai, K.; et al. *J. Natl. Cancer Inst.* **1993**, *85*, 785–93.
(20) Punnonen, K.; Hietanen, E.; Auvinen, O.; Punnonen, R. *J. Cancer Res. Clin. Oncol.* **1989**, *115*, 575–8.
(21) London, S. J.; et al. *J. Natl. Cancer Inst.* **1993**, *86*, 785–93.
(22) Chajes, V.; et al. *Int. J. Cancer* **1992**, *50*, 405–8.
(23) Hietanen, E.; Punnonen, K.; Punnonen, R.; Auvinen, O. *Carcinogenesis* **1986**, *7*, 1965–9.
(24) Bougnoux, P.; et al. *Breast Cancer Res. Treat.* **1992**, *20*, 185–94.
(25) Frank, C. J. Ph.D. Dissertation, The Ohio State University, Columbus, OH, 1994.

enzymes in oncogenesis at the cell membrane level suggests that membrane lipids may play a role in modulation of breast tumor growth.

Figure 6 demonstrates that a fiber-optic probe positioned above a normal tissue sample introduces minimal spectral distortion but that silica background becomes apparent when the much weaker scatter from diseased tissue is observed. The ability to use a fiber-optic probe imparts significant flexibility to the approach, since a surgeon or pathologist could easily point a fiber-optic probe at the tissue in question, and the spectrometer could be a few meters away. The sampling depth of a fiber probe positioned above the specimen will of course depend on tissue absorption and scatter but will be a few millimeters. The 6 × 1 needle probe inserted into the tissue can sample much deeper and is in principle no more invasive than existing biopsy techniques. The spectra of Figure 7 show clear differences between normal and diseased tissue, with the added information of spatial resolution of ~1 mm. The spectra of Figure 8 demonstrate that useful information is available even with a long length of fiber (50 ft) between the sample and the spectrometer. The efficiency and background of such probes are improving rapidly and several alternative designs are available.

A concern with any Raman technique applied to tissue is the possibility of radiation damage. CCD spectrometers are sufficiently sensitive that laser powers of a few milliwatts generate useful spectra. However, safety limits for living tissue exposure to laser light are not yet established and will vary with tissue type and spot size. Fiber-optic probes can reduce power density substantially (depending on design), but it is clear that radiation damage will have to be evaluated if a Raman technique is to be used in vivo.

ACKNOWLEDGMENT

The authors appreciate the assistance of Ted S. Gansler at Emory University, who provided several samples and pathology reports. Equipment loans from Chromex (Albuquerque, NM) and Detection Limit Technology (Laramie, WY) were very valuable. This work was supported by the National Science Foundation Division of Analytical and Surface Chemistry.

Received for review November 28, 1994. Accepted January 10, 1995.[⊗]

AC941135O

[⊗] Abstract published in *Advance ACS Abstracts,* February 1, 1995.